3D Printed Polypyrrole Microneedle Arrays for Electronically Controlled Transdural Drug Release

Joyce Huang

A thesis

submitted in partial fulfillment of the

requirements for the degree of

Master of Science

University of Washington

2020

Committee:

Rajiv Saigal, Chair

Susie Pun

Program Authorized to Offer Degree:

Bioengineering

University of Washington

Abstract

3D Printed Polypyrrole Microneedle Arrays for Electronically Controlled Transdural Drug Release

Joyce Huang

Chair of the Supervisory Committee:
Rajiv Saigal, MD Ph.D.
Assistant Professor
Neurological Surgery

The secondary injury causes further damage to neural cells, due to mechanisms of inflammation and cytotoxicity. Progression of secondary injury damage may be reduced by the administration of anti-inflammatory drugs. In order to allow local delivery of such drugs, while minimizing dural opening, we have created a Polypyrrole (PPy) microneedle array using micro-scale 3D printing technology that facilitates electronically controlled encapsulation and transdural release of drugs. The PPy microneedles demonstrated electronically controlled transdural release of steroid dexamethasone (Dexa) in a novel in vitro transdural model. Drug release capabilities of the device were then tested by electronic release of Dexa into an in-vitro model of activated BV2 microglia. After 72 hours of incubation, inflammation was reduced, as demonstrated by measured release of nitric oxide and Il-1b, a pro-inflammatory cytokine. These results demonstrate the feasibility of PPy microneedles for transdural delivery of anti-inflammatory drugs for spinal cord injury.

TABLE OF CONTENTS

LIST OF FIGURES

Chapter 1. INTRODUCTION

Spinal cord injuries (SCI) results in lasting disabilities with significant impacts on patent lives. In the United States, approximately 17,000 new cases occur each year, of which less than 1% make a complete recovery[1, 2]. Patients are often left with severe paralysis. Accumulated lifetime costs, including medical care and lost earnings can total nearly $40 million[3]. Despite increasing survival rates of spinal cord injury patients, the quality of life is still often poor.

The lasting damage of SCI may be attributed to the low rates of neural recovery in addition to the complex physiology and mechanism of SCI. The initial physical injury in SCI is followed by a secondary injury minutes later, and lasting up to months [4]. Secondary injury mechanisms of neuroinflammation[5], excitotoxicity[6], and ischemia[7] attribute to further damage of the injured spinal cord. Excitotoxicity caused by excess neurotransmitters, free radicals, reactive oxygen species, released as a result of the primary injury[8, 9] lead to deaths of surrounding uninjured cells. Released inflammatory factors stimulate inflammatory responses of surrounding glial cells, resulting in the release of proapoptotic factors and additional free radicals. Free radicals such as nitric oxide (NO) released by inflammatory microglia have been found to damage surrounding uninjured tissue [2]. Excessive NO induce apoptosis in nearby neurons. This secondary apoptotic neuron death has been observed at a distance from the injury site, for up to several weeks post-injury[9].

The current standard of care for SCI is early surgical decompression, along with optimizing perfusion to the spinal cord by maintaining arterial pressure [10] [11]. Blood, fragments of bone, and other tissues impinging on the spinal cord are surgically removed. Spinal

structures are stabilized using implanted screws and rods. Decompression surgery serves to significantly reduce further damage from spinal cord compression, but may not prevent the damage of the secondary injury. Patients generally then undergo physical and occupational therapy. However, patients with complete SCI often do not improve despite rehabilitation.

Recent works have investigated the combination of rehabilitation and electrical stimulation therapy. Epidural stimulation has been used in animal and human trials, with promising results [12-14]. In these studies, electrode arrays were implanted epidurally over the SCI lesion, and connected to a subcutaneous electrical pulse generator. Patients that underwent rehabilitation with epidural electrical stimulation were reported to have regained some voluntary movement abilities following treatment, even after the removal of electrical stimulus.

In order to maximize recovery, researchers have also conducted widespread research into pharmaceutical therapies. Many of these therapies aim to reduce further damage by targeting the secondary mechanisms of spinal cord injury. A variety of drugs with anti-apoptotic, anti-inflammatory, and anti-peroxidation properties have been tested for the treatment of secondary spinal cord injuries [15, 16]. Many drugs have shown promise in preclinical animal trials, however none have been approved for clinical applications. Steroids have been widely used in these studies due to their anti-inflammatory properties, the most extensively studied of which is methylprednisolone. In a randomized controlled trial, methylprednisolone was associated with a modest improvement in motor recovery after acute SCI [17, 18] However, the use of high dose steroids, such as methylprednisolone, is controversial in SCI due to the systematic side effects, such as sepsis and pneumonia [19]. Due to concern over adverse side effects and marginal neurological improvement, recent

guidelines recommended against methylprednisolone for treatment of SCI [20]. Consequently, there is no clearly beneficial pharmacotherapy for SCI.

The use of controlled local delivery may reduce side effects and improve efficacy. Local delivery may reduce off-target effects, while maintaining local concentration. Local controlled release also has the added benefit of allowing drugs to be delivered without need to cross the blood brain barrier. Many promising drugs, particularly large molecule and protein therapeutics, are restricted by their inability to cross the blood brain barrier that surrounds the spinal cord. These drugs are thus restricted to single bolus delivery through dural punctures. These restrictions have prompted several groups to develop intrathecal and intramedullary local controlled release [21-25]. However, the use of these systems require incisions of the dura, the protective sheath that encases cerebrospinal fluid (CSF) and the spinal cord. This approach of opening the dura adds risk of CSF leak, meningitis, and damage to the spinal cord itself. Thus, dural incisions should be avoided if possible. To minimize damage to the dura, researchers have developed a fast-gelling hydrogel that can be injected into the intrathecal space [26]. However, injection of the hydrogel also induces damage, albeit smaller, to the dura. Additionally, these intrathecal polymers may also reduce intrathecal space and impede CSF flow. Ideally, a drug delivery system would deliver locally into the intrathecal space with minimal damage to the dura, while not impeding neural functions.

Other proposed delivery methods include the application of drug delivery devices that allow external control of temporal release. These systems utilize conductive polymers, which encapsulate and release dopants during oxidation and reduction, respectively. One of the most common conductive polymers, polypyrrole (PPy) has been used in various studies for

drug release and implanted electrodes. *In vitro* and in vivo experiments found PPy biocompatible for use in the brain, supporting the growth of cerebral cortical cells [27]. Other studies utilized these characteristics of PPy to release dexamethasone (Dexa), an anti-inflammatory drug, to create coatings for neural interfacing electrodes [28, 29]. Dexa release from PPy was used to attenuate astrocyte reactivity [28, 29], and reduce glial scarring. Analysis of drug release from the device shows that PPy can be used to deliver drugs with precise timing via electrical stimulation. However, the implantation of these delivery systems also require incisions into the dura.

In this work, we describe a microneedle array for electronically controlled transdural delivery that may allow the use of electronically controlled delivery from PPy, while minimizing the need for incisions into the dura. The implanted electrode then allows the local delivery of neuroprotective or anti-inflammatory drugs. The microneedles may be placed during a decompression surgery. The implant may be placed epidurally, while piercing the dura to deliver drugs to the intrathecal space. Here, we will investigate the transdural and electronically controlled delivery of a model drug, dexamethasone phosphate using the PPy microneedles. Dexamethasone phosphate, an ionic prodrug of corticosteroid dexamethasone, is commonly used in electronically controlled drug release [28-31]. Dexamethasone phosphate is converted to Dexamethasone in serum. The delivery of dexamethasone phosphate has also been demonstrated to reduce neuroinflammation and subsequent apoptosis in *in vitro*[32] and animal models [15, 33]. Dexamethasone phosphate will be used here for transdural delivery through the PPy microneedles to attenuate *in vitro* neuroinflammation.

Chapter 2. EXPERIMENTAL

2.1 MICRONEEDLE FABRICATION

Microneedles were fabricated using three-dimensional photolithography (NanoScribe GnbH, NanoScribe). 10x10 arrays of conical microneedles with 500um height and 130um diameter, along with a 20um thick square base, were printed on plasma treated silicon wafers in IP-S resist (NanoScribe). Microneedles in the array were spaced at every 250um from point-to-point. Exposed microneedles were then developed in SU-8 Developer (Microchem) for 20 minutes, followed by cleaning in an isopropanol solution for 5 minutes. Following developing, microneedles were further cured under a UV flood light (ABM) of approximately intensity 11.5 lx for 90 seconds. Microneedle wafers were then diced into 7mm x 7mm chips each containing an individual microneedle array. Microneedle chips were coated on both surfaces by sputter coating (Evatec LLS EVO Sputter System) in 10nm chrome and 100nm gold. The sputtered coating was allowed to coat the sides, and forming electrical connections between the top and bottom surfaces. Electrical connections were made by soldering to the surface opposite the microneedles. The metal coated microneedle electrodes were then deposited in PPy following the protocol above. Flat electrodes were made similarly through dicing and sputter coating silicon, followed by soldering and Dexa PPy electrodeposition.

2.1 PPy Deposition

Microneedle electrodes to be coated in PPy were submerged in a solution of 0.2M pyrrole (Pyr, ThermoFisher) and 0.2M sodium dodecylbenzenesulfonate (NaDBS, ThermoFisher) in water across a platinum anode. A blank (no drug) adhesion layer was first deposited by the application of 1mA across the Pyr solution for 2 minutes. The electrode was then submerged in a Pyr solution for the treatment layer, and subjected to 2mA of current for 4minutes. Treatment layer for the blank PPy was again deposited in fresh 0.2M Pyr, 0.2M NaDBS solution. Treatment layer of the Dexamethasone PPy (Dexa PPy) was deposited in a solution of 0.2M Pyr, 100mg/ml dexamethasone phosphate (Dexa), without NaDBS. Excess and unbound Pyr monomers and dopants were then removed by washing in 0.9M phosphate buffered saline (PBS, Gibco) three times on a rotating shaker for five minutes each. The process of microneedle fabrication and PPy deposition are shown in figure 2.1.

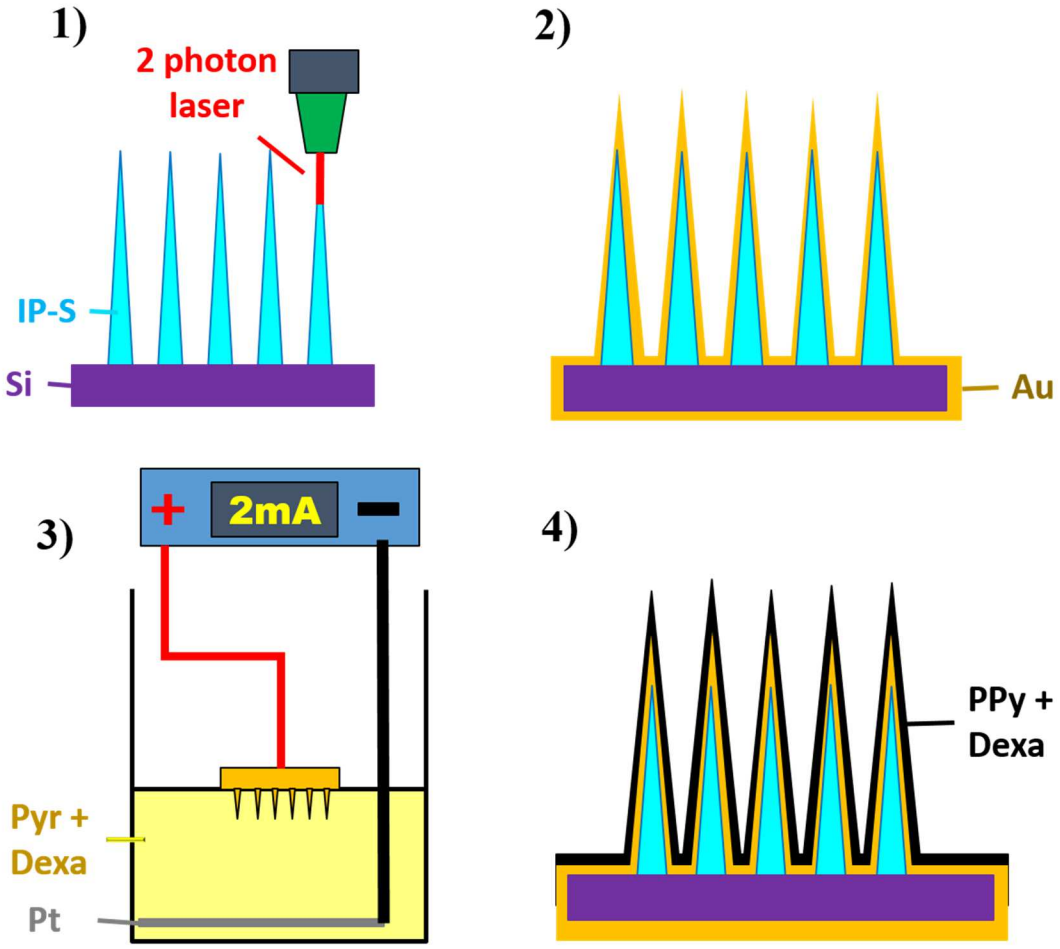

Figure 2.1. Summary Schematic of microneedle fabrication and PPy deposition process. 1) 3D photolithography of microneedles on silicon substrate using Nanoscribe. 2) Sputter coating of microneedle surface in gold. 3) Electrodeposition of Dexa PPy on microneedle surface in Pyr and Dexa solution. 4) Cross section of completed PPy microneedles.

2.2 MICRONEEDLE ARRAY MECHANICAL CHARACTERIZATION

The mechanical strength of the fabricated microneedles was tested using an in situ indentor (Alemnis) under SEM (Thermofisher Apreo S). The microneedles were indented using a stainless-steel flat punch tip. Indentation of the microneedles occurred at 17.3nm/sec until 10um total displacement. Microneedles were then also indented at 75nm/sec until 20um, 150nm/sec until 35um, and 500nm/sec until 35um. New microneedles were used for each indentation. Resultant load at each displacement point was recorded.

2.3 *IN VITRO* TRANSDURAL RELEASE

Transdural release assays from the PPy microneedles, as well as controls, were performed in a custom transwell *in vitro* model (fig. 2.2a,c). Transwell inserts were designed and 3D printed in PLA to allow suspension of a dural substitute (DuraMatrix) over solution within a 12 well plate. The bottom and outside surfaces of the insert were sputter coated in 10nm of chrome and 100nm of gold to create a counterelectode for stimulated release. A square of suturable dura substitute was then fixed to bottom opening of the transwell insert using cyanoacrylate gel (Loctite). The fixed transdural insert was then allowed to dry, then the dura hydrated with 400ul of PBS. Transdural inserts were placed into wells over 1.6ml of PBS. Microneedles were applied epidurally over the dura substitute using manual pressure. Flat electrodes were placed and stimulated similarly.

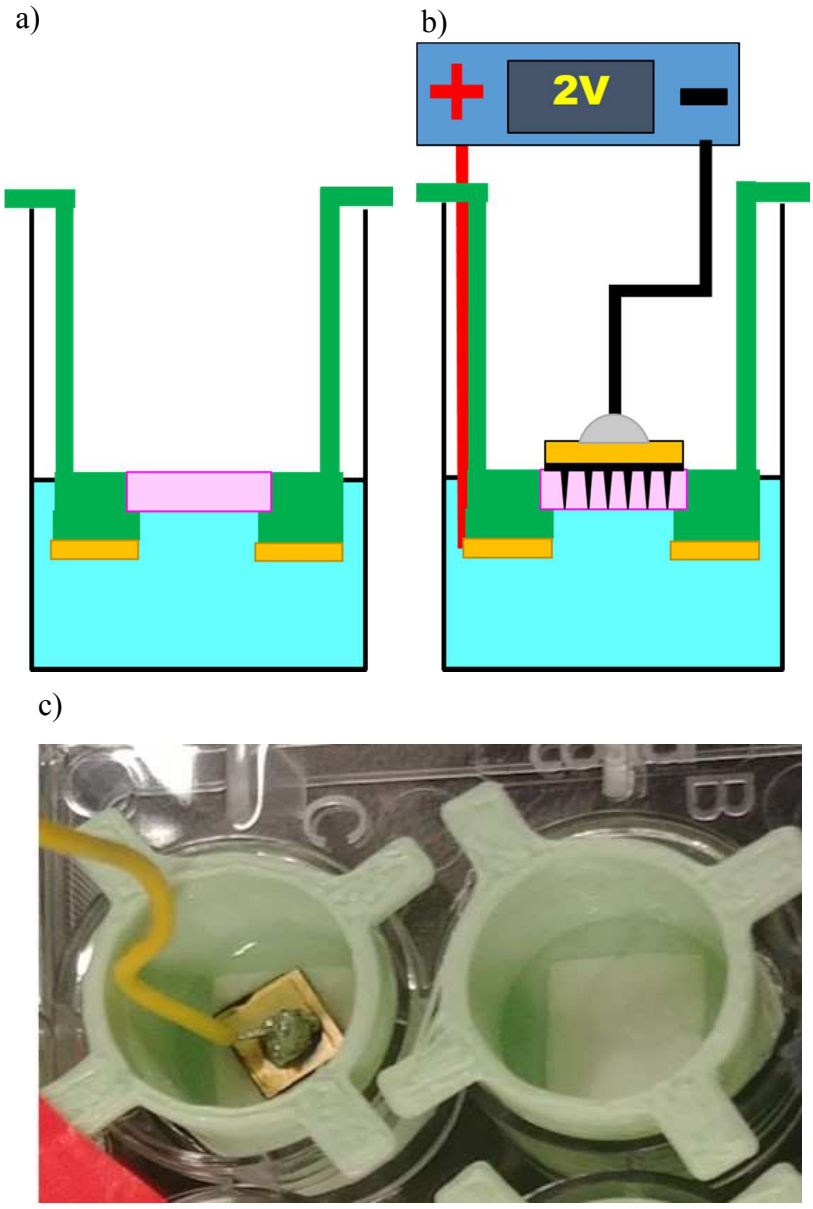

Figure 2.2. *In vitro* transdural Model.

a) Schematic of transdural model in solution. Artificial dura is suspended over solution in 3D printed PLA transwell insert. b) Schematic of microneedle application to the transdural model. Bottom surface of the insert was coated in gold to form a conductive surface for electrical stimulation through the solution. Microneedles were applied to the insert epidurally. c) Image of microneedles in the *in vitro* transdural model.

Electrical stimulation could then be applied through the microneedle to the coated insert as an electrode (fig. 2.2b) . Stimulated release samples underwent 10mins of direct current (DC) at -2V or cyclic voltammetry (CV) of 100mV/s from -1V to 1V. Groups of n=6 microneedle arrays were stimulated under DC for 10 minutes in order to allow quantification of maximum release. However, due to apparent cell stress and death from long durations of DC stimulation, the DC stimulated release was also performed at a reduced duration of 2 minutes. Drug in solution were applied to epidural and subdural controls by pipetting over or below the dural insert, respectively. 200ul of Dexa solution with a concentration of 50ug/ml was used in controls.

An SEM image of the microneedles was taken before and after the transdural placement. To allow for SEM imaging, electrical connections to the microneedle array must be removed, thus microneedles imaged immediately after PPy deposition were not subsequently used for implantation and transdural release. Another microneedle array used for transdural implantation and release was similarly processed and imaged in SEM.

2.4 Dexamethasone Quantification

Dexa phosphate (Dexa) released was quantified using high pressure liquid chromatography (HPLC) and mass spectrometry (MS). Predisolone phosphate (Pred,) was added to each sample as an internal standard, prior to processing. Each sample received prednisolone phosphate to a final sample concentration of 2ug/ml. Drug release samples were passed through a 0.2um PVDF filter prior to autosampler injection. Aqueous and organic phases used were 10mM ammonium acetate in water and methanol, respectively. The compounds

were separated in chromatography through a Zorbax Extend C-18 3.5um HPLC column (Agilent), at a flow rate of 0.3mL/min. Dexa and Pred ions of m/z 471.1500 and 439.1043, respectively, were extracted. The Pred ion was isolated with a peak at approximately 2.00mins, and the Dexa ion at approximately 3.75mins. For each compound, fragments of m/z 79 and 97 were isolated in negative ion mode, and used for quantification. Dexa in the solution was quantified by comparison against a calibration curve of Dexa in PBS, with similarly added Pred. Samples were quantified using the ratio of Dexa to the constant concentration of internal standard Pred.

2.5 *IN VITRO* NEUROINFLAMMATION ASSAY

Bioactivity of electrically released drug was tested in an *in vitro* neuroinflammation model, in which drugs were released into wells of activated BV2 murine microglia. Healthy BV2 cells were seeded in 12 well plates at a density of 100,000 cells/well, in 1.6mLs of Dulbecco's modified eagle media (DMEM, Gibco) with 4.5g/L D-glucose, 584mg/L L-glutamine, and 110mg mg/L sodium pyruvate (Invitrogen). The DMEM was supplemented with 5% fetal bovine serum (Invitrogen) and 2% anti-mycotic/anti-biotic (Invitrogen). Following seeding, the cells were incubated at 37 overnight to allow for settling and adhesion. Cells in activated treatment groups were activated by the replacement of media with fresh DMEM containing 0.005% interferon gamma (Ifn-γ, Invitrogen) and 1% lipopolysaccharide (LPS, ThermoFisher). Unactivated controls received normal fresh DMEM. Cells were then incubated for 1 hour before application of treatment in groups of n=6, in order to simulate realistic conditions in which there is a duration between traumatic SCI occurrence and access to treatment.

Treatment was applied transdurally from microneedles into the cell media though the transdural insert model as previously described in the *In Vitro Transdural Release* section. Diagrams of experimental conditions can be found in Fig. 3. Microneedles were similarly applied manually, then underwent a potentiostatic or cyclic electrical stimulation. Direct current potential was applied for only 2 minutes to minimize electrical imbalance applied to the cells, while delivering sufficient drug to achieve therapeutic effect. Cyclic voltammetry was applied for 15 cycles, equating to 10 minutes. Epidural drug solution controls were similarly applied to the neuroinflammation model by pipetting over the transdural insert. In addition, a subdural solution control was introduced to the neuroinflammation studies in which the Dexa solution is applied directly to the cell media, bypassing the transdural insert.

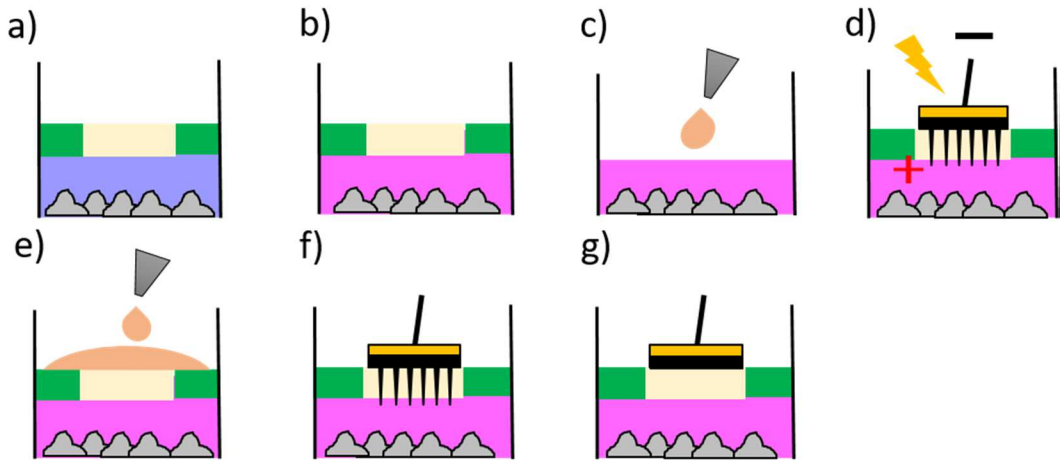

Figure 2.3. Simplified diagrams of *in vitro* neuroinflammation experimental conditions.

Simplified diagrams of *in vitro* neuroinflammation experimental conditions: a) unactivated BV2 microglia, b) **Error! Bookmark not defined.**activated BV2 microglia without treatment, c) subdural Dexa solution treatment of activated microglia, d) electrically stimulated PPy microneedles (Dexa or blank), e) epidural drug solution, f) non-stimulated Dexa PPy microneedles, and g) stimulated flat PPy release.

Following 3 days of incubation, cell media was assayed for markers of inflammation. Free radical nitric oxide (NO) was quantified using a Griess reagent kit (Invitrogen) that detects NO reduced to nitrites in cell media[34]. Colorimetric NO quantification was performed following the protocols provided in the Griess reagent kit. Pro-inflammatory cytokines were quantified using a Luminex Magpix Multiplexing assay (Millipore). Cytokines quantified include interleukin-1-beta (IL-1β), interleukin-6 (IL-6), and tumour necrosis factor alpha (TNF-α). Cells treated in the CV stimulated experiment were additionally quantified for the release of monocyte chemoattractant protein 1 (MCP-1). The Luminex multiplexing assays were performed following the protocol provided in the kit.

Cell viability was measured using an MTS assay (CellTiter 96® AQueous One Solution Cell Proliferation Assay, Promega). Cells received 1ml of fresh DMEM, along with 200ul of MTS reagent, then were incubated for 1 hour. The incubation was followed by detection of absorbance at 490nm. The MTS absorbance in each group was normalized to the absorbance of the unactivated group.

2.6 Statistical Analysis

Statistical analysis was performed using SPSS Statistics 25 (IBM). Sample groups were checked for normal distribution using a Shapiro-wilk test, then checked for homogeneity of variances using Leven's test. One-way ANOVA with post-hoc Bonferroni analysis was performed on experiments with 3 or more groups, and homogeneity of variances. Experiments without homogeneity of variances were instead assessed using a post-hoc Games-Howell test. Student's T test was performed on experiments with 2 groups.

Chapter 3. RESULTS AND DISCUSSION

3.1 MICRONEEDLE MECHANICAL CHARACTERIZATION

To characterize the mechanical strength of the microneedles, we subjected the microneedles to stress testing under a nanoindenter. The microneedles were compressed in the indenter under a constant rate of displacement, while visualized using SEM (Appendix A). Under SEM visualization, it was apparent that the microneedles experienced bending rather than compression under the force of the indenter (fig. 3.1). Due to bending and change in contact surface area, we were unable to quantify mechanical strength of the microneedle.

However, load vs displacement curves produced allowed us to qualitatively assess the elasticity of the microneedles. On application of downward force, the tip of the microneedle bends, but recovers as the force is removed. The magnitude of plastic deformation is dependent on the rate of displacement. The magnitude of deformation increased as the rate of displacement was increased. The difference in deformation can be seen in the graphs displaying displacement rates of 150nm/sec and 500nm/sec both to a maximum of 35um. On graphs displaying experienced load of max displacement 20um and greater (fig. 3.2) , the point of bending can be seen at approximately 4um, where the rapid increase in load is reduced as the tip is bent. A secondary shoulder can be seen in the load of 500nm/sec displacement.

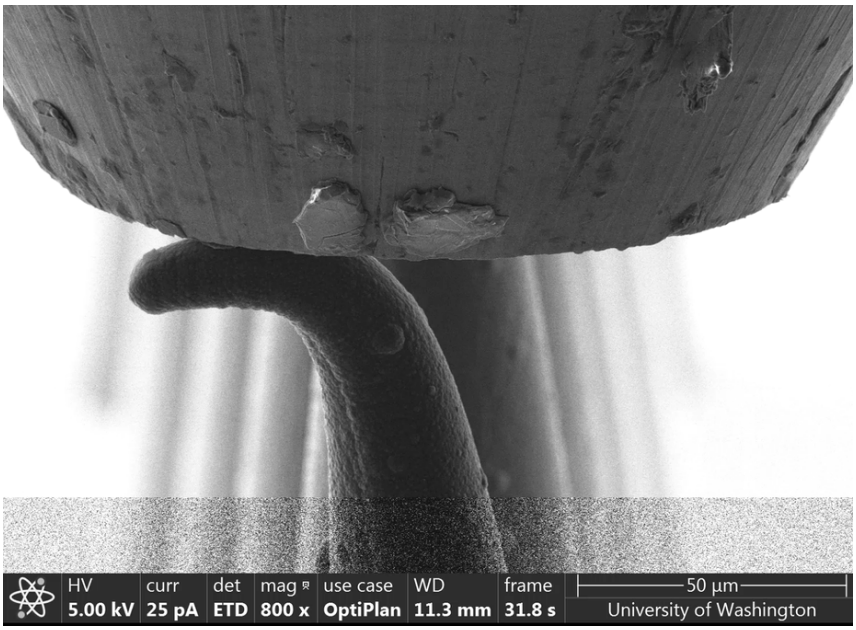

Figure 3.1. SEM image of PPy microneedle under compression stress testing.

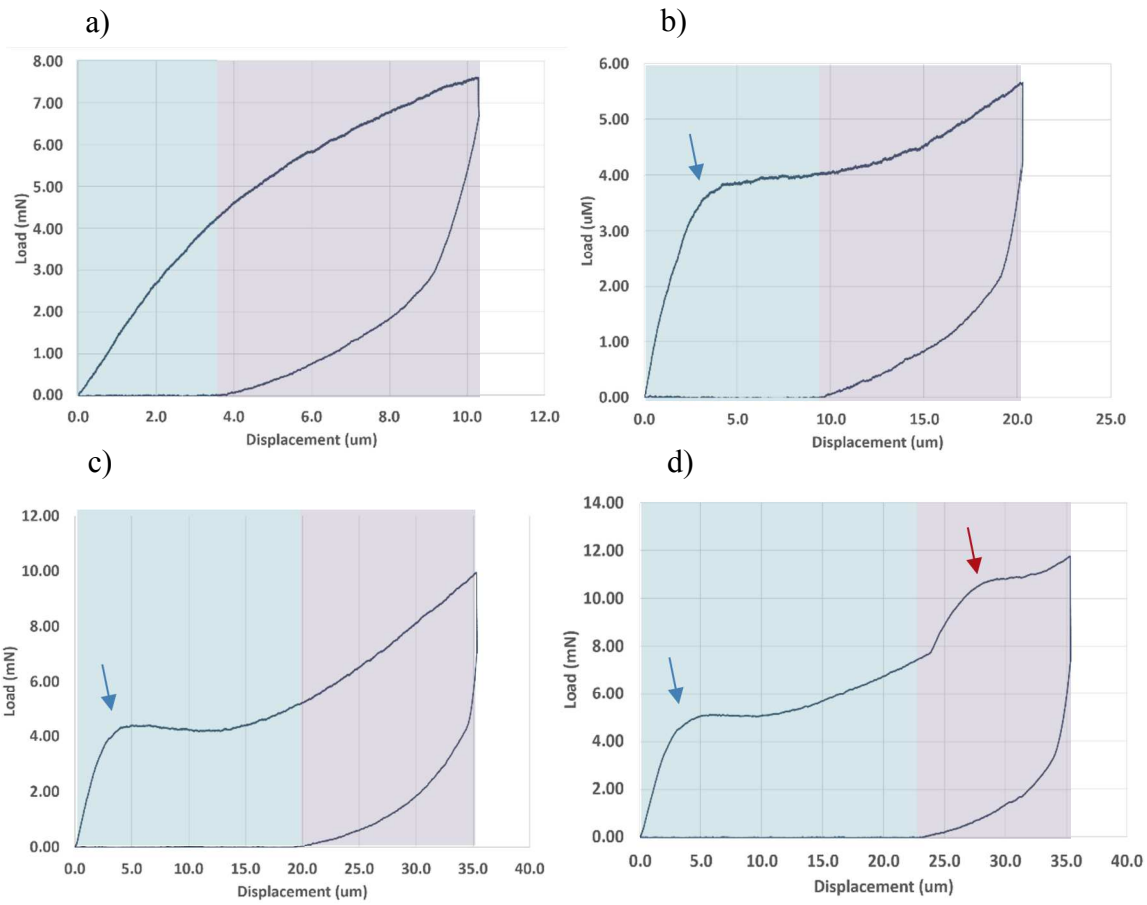

Figure 3.2. Load vs Displacement curves of microneedle indentation.

Resultant load curves of microneedle tip displacement for a) 17.3nm/sec to a max displacement of 10um, b) 75nm/sec to a max displacement of 20um, c)150nm/sec to a max displacement of 35um, and d) 500nm/sec to a max displacement of 35um. The blue arrow indicates point of bending at approximately 4um. An additional bending point in the 500nm/sec displacement is indicated by a red arrow. Area displaying elastic recovery is shaded in blue, area displaying plastic deformation is shaded in purple.

3.2 *IN VITRO* TRANSDURAL DRUG RELEASE

Drug release from 10x10 arrays of Dexa PPy microneedles was tested in a custom designed *in vitro* model to demonstrate transdural release. In this model, the microneedles were used to puncture artificial dura at the bottom of a transwell insert, and release into solution below. Electrical stimulation may then be applied through the solution. In addition, transdural release was tested in microneedles without electrical stimulation, as well as microneedles without drug, and from epidurally applied Dexa solution (fig. 3.3). As expected, PPy microneedles without drug did not result in subdural Dexa release. Similarly, epidural Dexa solution resulted in no subdural Dexa, indicating that Dexa released epidurally does not undergo passive diffusion through the transdural insert. Quantification of subdural solution found that Dexa PPy microneedles that experience 10minutes of -2V potentiostatic stimulation resulted in a significantly higher amount of transdural Dexa release. The use of Dexa PPy microneedles appears to allow transdural release of Dexa. However, similar Dexa PPy microneedles without electrical stimulation resulted in very little transdural Dexa release, illustrating electrical control of Dexa release from Dexa PPy microneedles . The ability for electrically stimulated release then allows precise temporal control of drug release, with external control throughout duration of implantation. Along with local implantation for transdural release, the DexaPPy microneedles demonstrate capability for temporal and spatial control of drug delivery to the spinal cord.

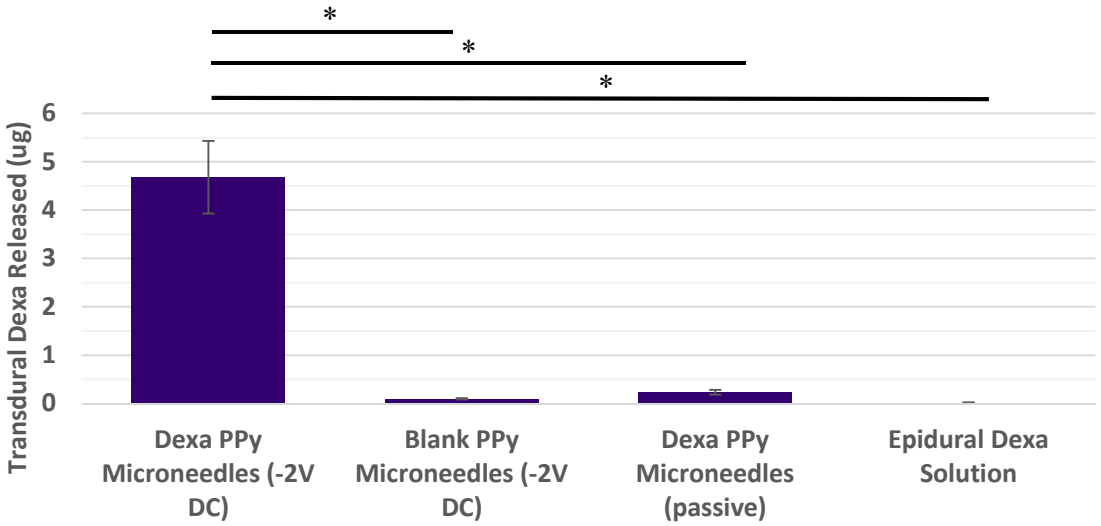

Figure 3.3. Quantified transdural release from DC stimulated Dexa PPy microneedles. Mass of Dexa in subdural solution following transdural release using DC stimulated Dexa PPy microneedles, DC stimulated blank PPy microneedles, non-stimulated (Passive Dexa PPy microneedles, and epidural Dexa stimulation. (* $p < 0.05$).

However, the current through PPy microneedles s was observed to decrease over the 10 minutes of stimulation, ultimately reaching approximately 0 at about 10 minutes. The decrease in current suggests a decrease in conductivity of the PPy, which occurs as a result of overoxidation of PPy. Along with over oxidation, application of a similar DC potential for such a long duration to a cellular environment may induce stress in cells. Thus, in order to adapt the release process to a cellular neurinflammation model, the duration of stimulation was reduced to 2 minutes. Transdural drug release from the Dexa PPy microneedles with 2 minutes of electrical stimulation was similarly quantified in the *in vitro* model. Unsurprisingly, reduced duration electrical stimulation resulted in lower amounts of drug release (fig. 3.4). The decreased stimulation reduced transdural drug release by approximately 60% to a total of 2ug.

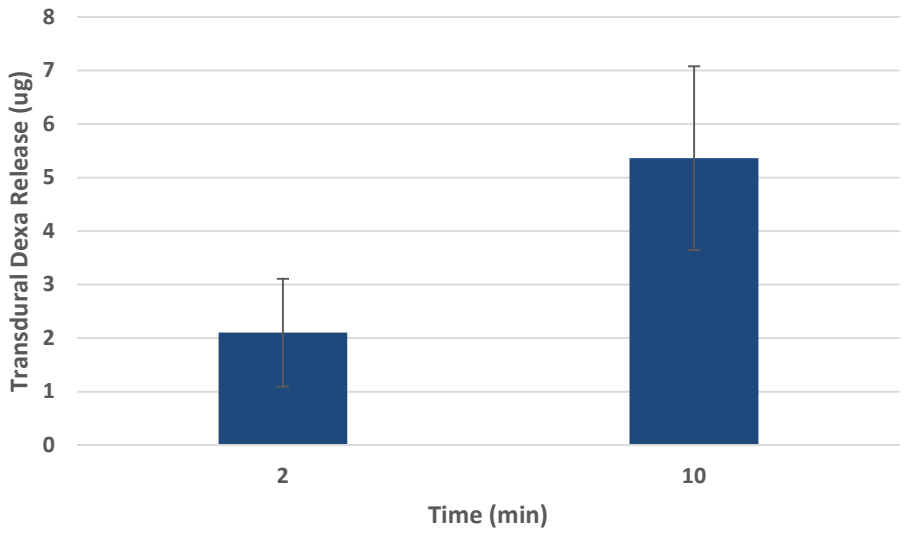

Figure 3.4. Quantified transdural Dexa release from DC stimulated Dexa PPy microneedles at 2mins and 10 mins.

Alternatively, we also explored stimulation of the DexaPPy microneedles using cyclic voltammetry in order to both reduce over-oxidation of the PPy, as well as allow charge balancing when stimulating in a cellular environment. The drug release was similarly performed in the *in vitro* transdural model. However, a cyclic potential of 100mV/s from -1V to 1V was applied. The CV stimulation was applied for 15 cycles, equating to 10 minutes of stimulation. The peak current throughout the CV stimulation remained level, indicating a lack of over-oxidation as seen in long duration DC stimulation. The ability to maintain PPy conductivity suggests that CV stimulation may be applied for durations extending beyond 15 cycles, for possibly higher amounts of drug release in future works. Ten minutes of CV stimulated release from Dexa PPy microneedles resulted in an average of 18.03ug of transdural Dexa release (fig. 3.5). The CV stimulated Dexa release is, however, highly variable. The variability may be attributed to

variable release from PPy. Nevertheless, all but one sample achieved a minimum of 3ug Dexa release.

Flat DexaPPy electrodes and Blank PPy microneedles were also tested for transdural release with CV stimulation. Neither resulted in measurable transdural Dexa release. The lack of transdural Dexa release from Flat Dexa PPy with stimulation demonstrates inability of Dexa to cross the transdural well through electrical forces alone. The lack of electrically driven transdural release suggests that microneedles play a role in allowing Dexa to cross the membrane.

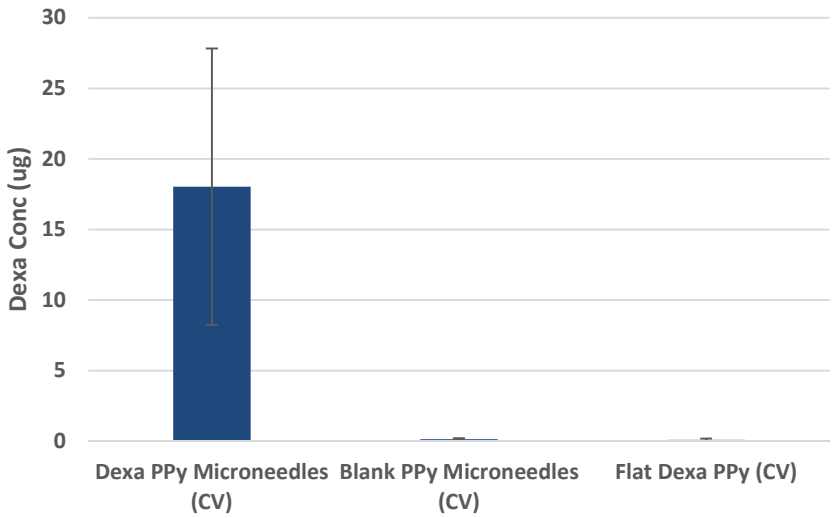

Figure 3.5. Quantified subdural Dexa release from CV stimulated Dexa PPy microneedles. Subdural Dexa is quantified following transdural release from CV stimulated Dexa PPy microneedles, CV stimulated Dexa PPy microneedles, and CV stimulated Flat Dexa PPy.

SEM imaging of the microneedles before and after implantation into the dura insert demonstrate durability of the microneedles against the artificial dura membrane (fig. 3.6). Representative SEM images were taken of a microneedle array following PPy deposition. While some microneedles experience slight bending prior to implantation, most display a sharp peak.

Following implantation, microneedles experience some blunting, as well as slight hooking of the tip, however, most microneedles maintained structural integrity through implantation and drug release.

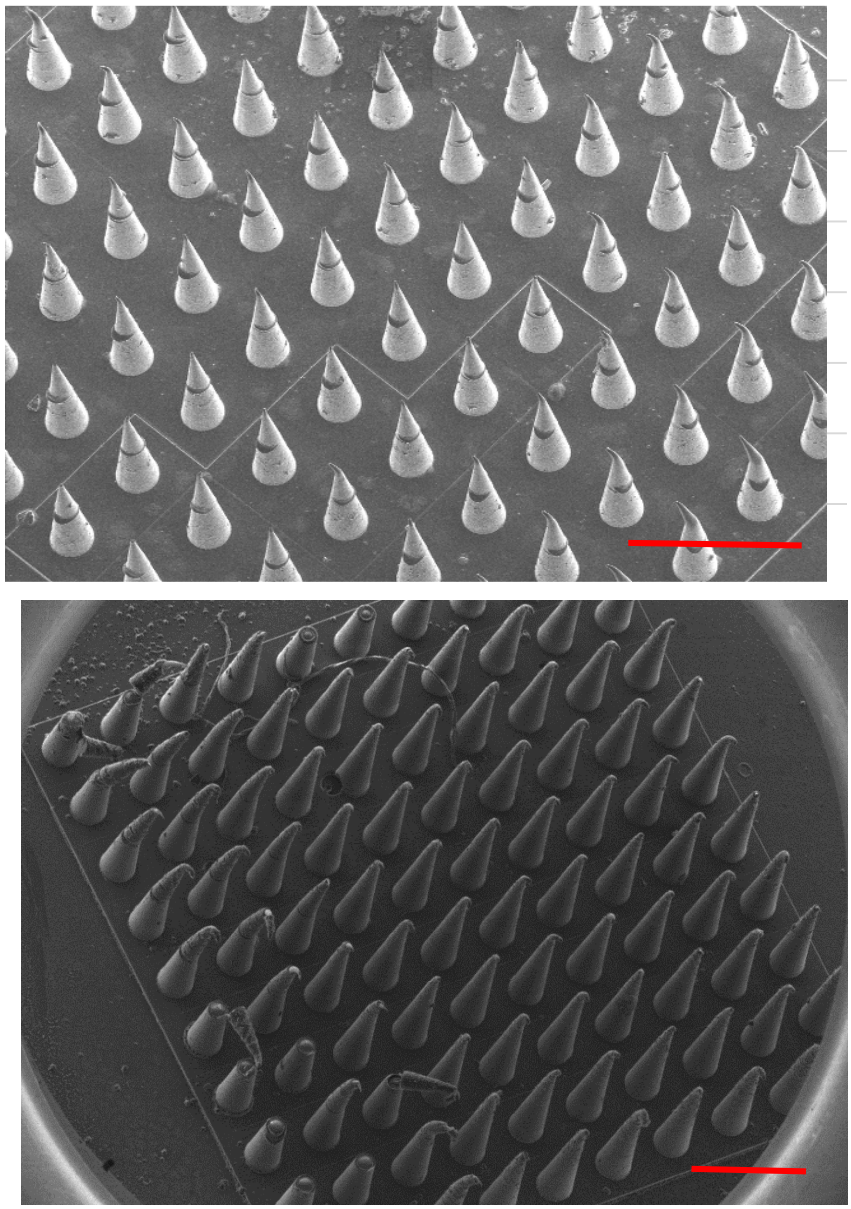

Figure 3.6. SEM images of PPy microneedles prior to and following insertion into dura. Top: microneedle array of 500um height and 130um diameter, prior to implantation in the transdural insert. Bottom: microneedle array of 500um height and 130um diameter microneedle array following implantation into transdural insert. Red bar indicates 500um length.

3.3 *IN VITRO* NEUROINFLAMMATION ASSAY

3.3.1 *DC Stimulated Release*

Transdural Dexa release from the microneedles was similarly tested in a neuroinflammation assay *in vitro*. BV2 Microglia cells were cultured in the wells of the transdural release model, and activated for inflammation using Ifn-γ and LPS. Shortly following activation, the cells received treatment. Cells were treated with subdural Dexa solution, DC stimulated Dexa PPy microneedles, epidural Dexa solution, non-stimulated Dexa PPy microneedles, and DC stimulated blank PPy microneedles. Additional control groups of unactivated cells, and activated but untreated cells were also included. After three days of incubation, the cells are assayed for NO release, inflammatory cytokine release, and cell viability. The release of NO and cytokines were normalized to the quantified cell viability in order to account for cell death or changes in rate of proliferation resultant of the treatments.

The relative cell viability of the treated cells was quantified using an MTS assay. The MTS assay is used for indirect quantified cell viability by measuring the metabolism of the MTS compound by mitochondrial dehydrgenases[35]. On analysis of cell viability (fig. 3.7a), it was noted that the group treated with DC stimulated Dexa PPy microneedles saw a significant decrease in cell viability. The subdural Dexa group saw slight decreases in viability, though not significant. The decrease in metabolism of MTS may indicate a decrease in proliferation rate in Dexa treated cells. However, the furthered decrease of cell viability in the DC stimulated Dexa PPy microneedle group may also indicate cell death as a result of the prolonged DC stimulation. Further experimentation may be required to determine the cause for decrease in cell viability.

The relative cell viability results were used to normalize the release of free radical NO and pro-inflammatory cytokines IL-1β, IL-6, and TNF-α. Normalized NO (fig. 3.7b.) saw a significant decrease in cells treated with subdural Dexa solution, demonstrating decrease of NO in Dexa treated microglia. Cells treated with DC stimulated Dexa PPy microneedles experienced a similar decrease in NO release, through electrically stimulated transdural release of Dexa. Groups of epidural Dexa solution, passive release from Dexa PPy microneedles, and DC stimulated Blank PPy microneedles did not demonstrate the same decrease. These results correspond with previous transdural release quantification, in which only stimulated Dexa PPy microneedles resulted in transdural Dexa release.

However, the release of pro-inflammatory cytokines did not experience similar patterns. The quantification of IL-1β, IL-6, and TNF-α show reduced total release in groups treated with DC stimulated Dexa PPy microneedles, but following normalization to cell viability (fig. 3.7c,d,e), the decrease can no longer be seen. Thus, the reduction in the release of pro-inflammatory cytokines may not be attributed to the attenuation of neuroinflammation, but may be attributed to microglia death. While decrease in NO release suggest promise in attenuation of neuroinflammation by DC stimulated Dexa PPy microneedles, further studies are required to investigate treatment effect on cellular stress and the release of pro-inflammatory cytokines.

a)

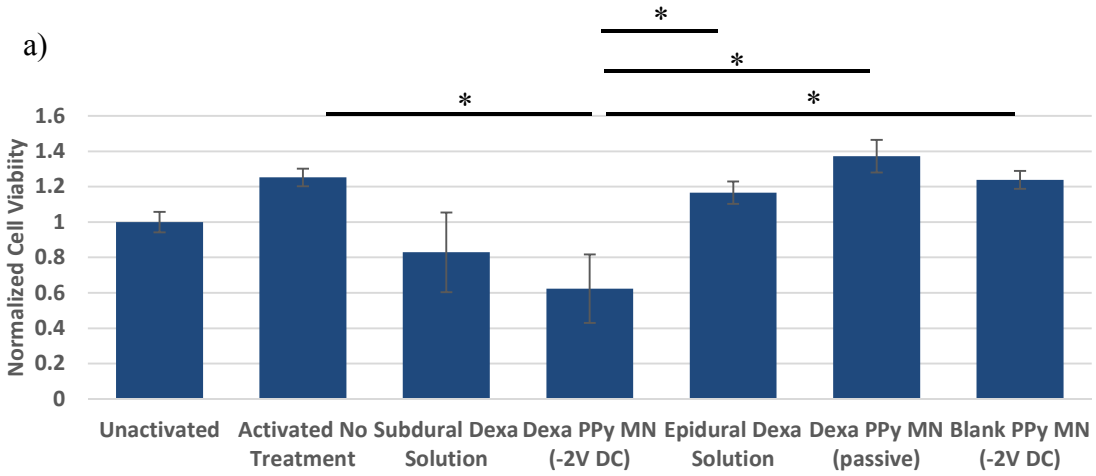
*
*
*
*
1.6
1.4
1.2
1
0.8
0.6
0.4
0.2
0
Normalized Cell Viability
Unactivated
Activated No Treatment
Subdural Dexa Solution
Dexa PPy MN (-2V DC)
Epidural Dexa Solution
Dexa PPy MN (passive)
Blank PPy MN (-2V DC)

b)

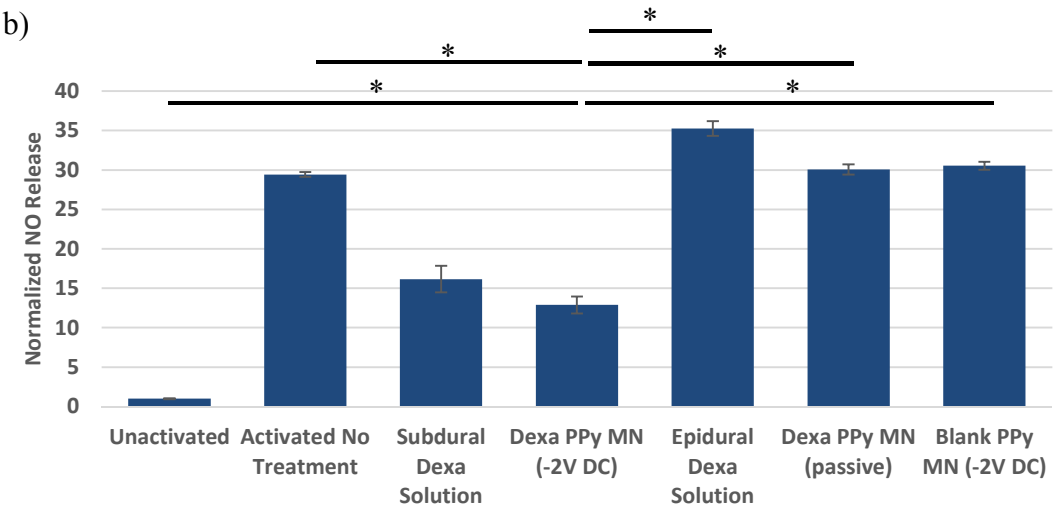
*
*
*
*
40
35
30
25
20
15
10
5
0
Normalized NO Release
Unactivated
Activated No Treatment
Subdural Dexa Solution
Dexa PPy MN (-2V DC)
Epidural Dexa Solution
Dexa PPy MN (passive)
Blank PPy MN (-2V DC)

c)

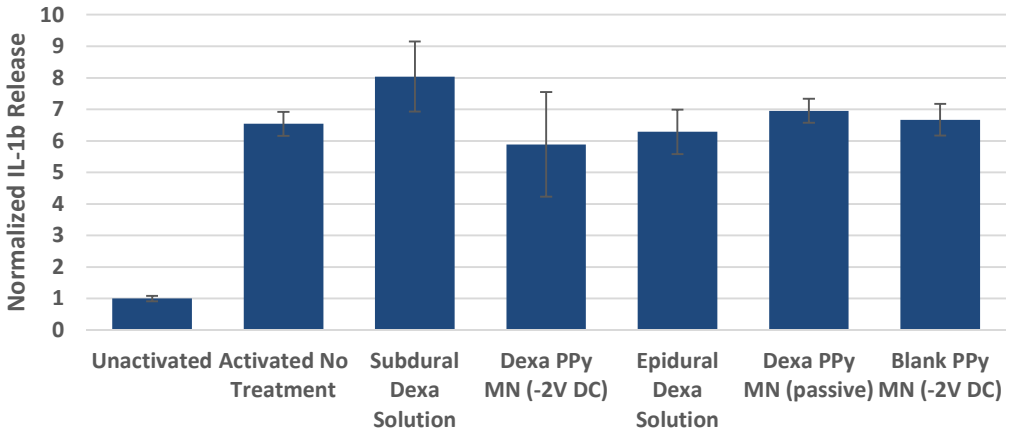
10
9
8
7
6
5
4
3
2
1
0
Normalized IL-1b Release
Unactivated
Activated No Treatment
Subdural Dexa Solution
Dexa PPy MN (-2V DC)
Epidural Dexa Solution
Dexa PPy MN (passive)
Blank PPy MN (-2V DC)

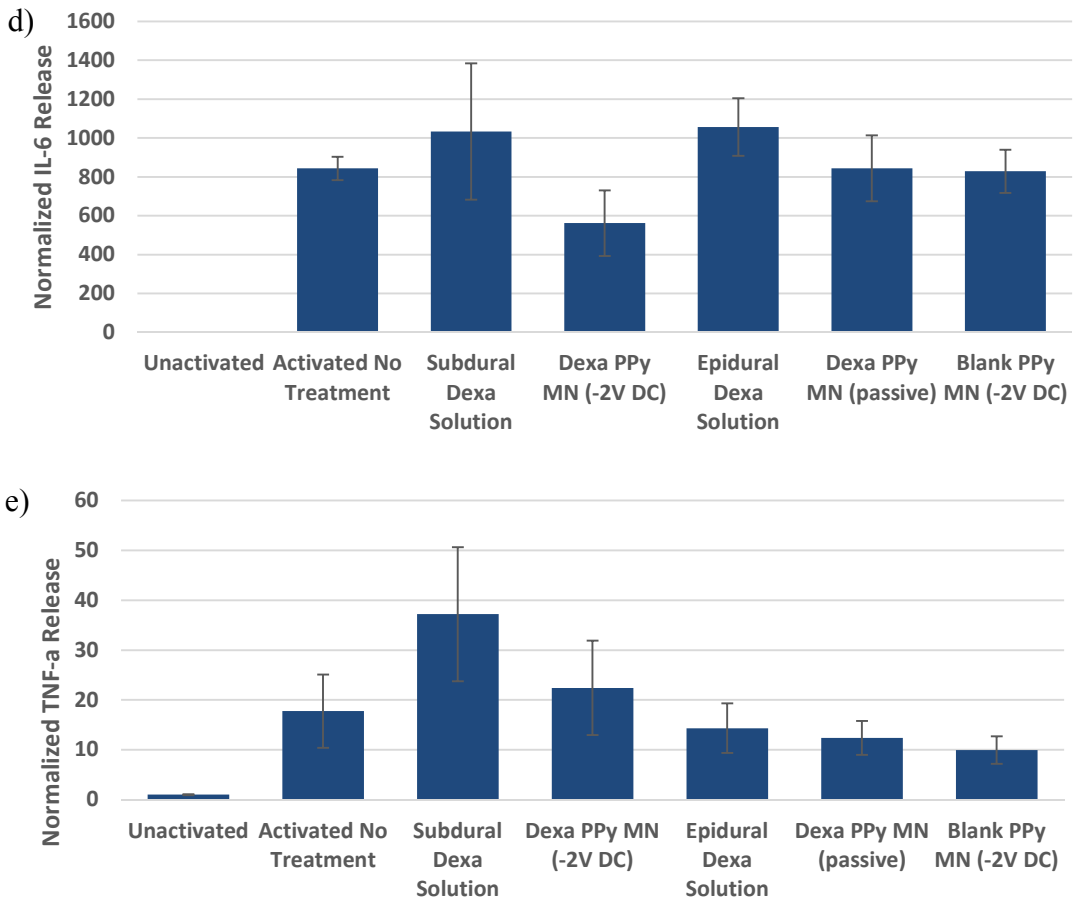

Figure 3.7. Neuroinflammation assays following transdural treatment of DC stimulated Dexa PPy microneedles.

a) Normalized cell viability as quantified using MTS colorimetric MTS metabolism. b) Release of NO, c) IL-1β, d) IL-6, e) TNF-α normalized by amount of viable cells quantified by MTS metabolism. (* $p < 0.05$ vs DC stimulated Dexa PPy microneedles)

3.3.2 *CV Stimulated Release*

The attenuation of neuroinflammation was similarly tested in CV stimulated Dexa PPy microneedles. Similar controls as previous were used, with the addition of a CV stimulated flat Dexa PPy electrode. Following the three day incubation, NO and pro-inflammatory cytokines IL-1β, IL-6, TNF-α, and MCP-1 were quantified using Griess and Luminex assays. Cell viability was again quantified using an MTS assay.

MTS relative cell viability quantification (fig. 3.8a) of CV stimulated Dexa PPy stimulated cells did not see the same decrease as previously seen in the DC stimulated treatment group. Instead, cell viability of the CV stimulated Dexa PPy microneedles group was increased compared to that of the controls. No groups in this experiment saw a decrease in cell viability, as measured by MTS metabolism, compared to that of unactivated cells.

Quantified release of inflammatory markers were then normalized to the amount of viable cells as measured using the MTS assay. NO release from the treated microglia, normalized for viable cells (fig. 3.8b), saw a reduction in the CV stimulated Dexa PPy microneedles treatment group. Subdural Dexa solution treated microglia experienced a similar reduction in normalized NO release. Activated microglia treated with CV stimulated flat Dexa PPy, epidural Dexa solution, non-stimulated Dexa PPy microneedles, or CV stimulated blank PPy microneedles did not see similar reductions in NO release. These treatment groups had previously been demonstrated to result in no transdural Dexa release, which likely correspond to the lack of reduction in the neuroinflammation marker. Surprisingly, the groups of CV stimulated flat PPy and blank PPy microneedles were seen to result in a slight increase in NO release. This increase may indicate a mechanism of increases in inflammation as a result of the stimulation parameters, which in the CV stimulated Dexa PPy microneedles is reduced by Dexamethasone treatment.

Normalized release of pro-inflammatory cytokines IL-1β, IL-6, and MCP-1 (fig. 3.8c,d,e) show similar patterns of decrease from microglia treated with CV stimulated Dexa PPy microneedles (fig). IL-1β, IL-6, and TNF-α (fig. 3.8f) saw a pattern of decrease in the CV stimulated Dexa PPy microneedles treated microglia. The release of MCP-1 display a similar pattern to that of NO. Treatment of CV stimulated Dexa PPy microneedles resulted in a greater decrease in the release of MCP-1, while controls of CV stimulated flat Dexa PPy, epidural Dexa solution, non-stimulated Dexa PPy microneedles, and CV stimulated blank PPy microneedles did not see the same decrease. The reduction of inflammatory cytokines, as well as NO, suggest that CV stimulated Dexa PPy microneedles may be used transdurally to attenuate neuroinflammation. Further investigations may be required to study the effect of the treatment on the signal transduction pathways of each cytokine.

a)

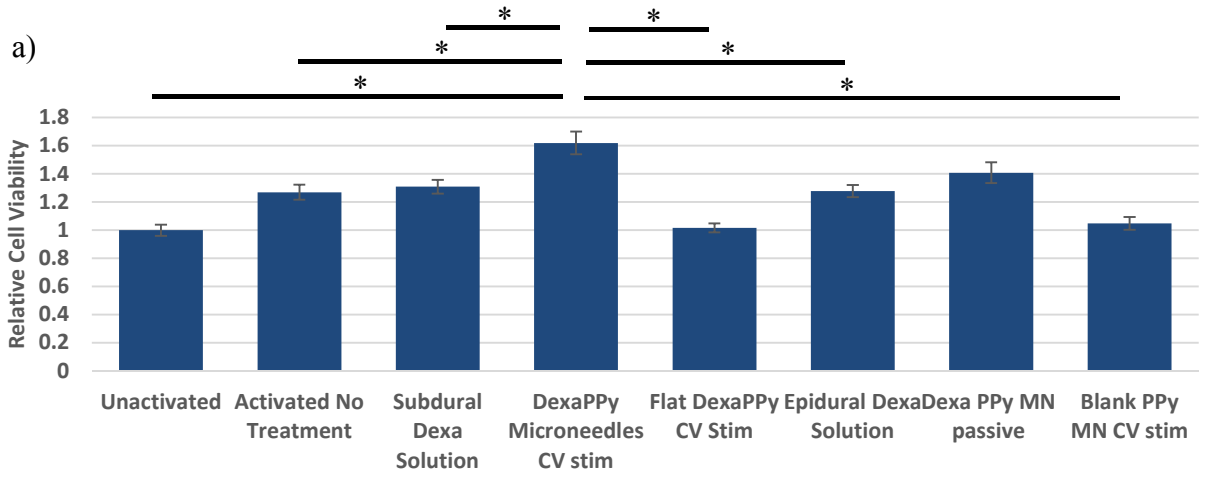
Relative Cell Viability
1.8
1.6
1.4
1.2
1
0.8
0.6
0.4
0.2
0
Unactivated
Activated No Treatment
Subdural Dexa Solution
DexaPPy Microneedles CV stim
Flat DexaPPy CV Stim
Epidural Dexa Solution
Dexa PPy MN passive
Blank PPy MN CV stim

b)

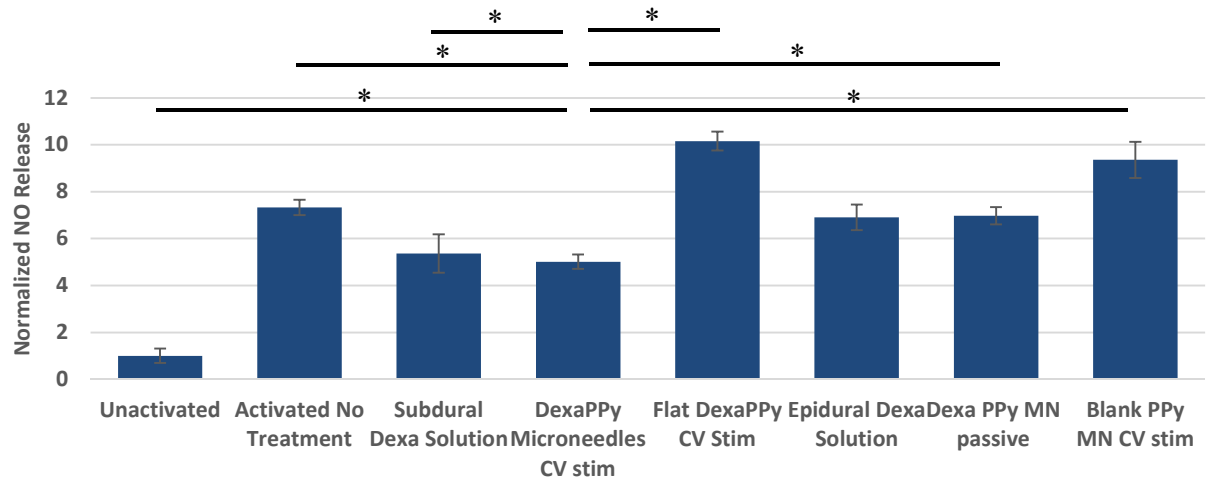
Normalized NO Release
12
10
8
6
4
2
0
Unactivated
Activated No Treatment
Subdural Dexa Solution
DexaPPy Microneedles CV stim
Flat DexaPPy CV Stim
Epidural Dexa Solution
Dexa PPy MN passive
Blank PPy MN CV stim

c)

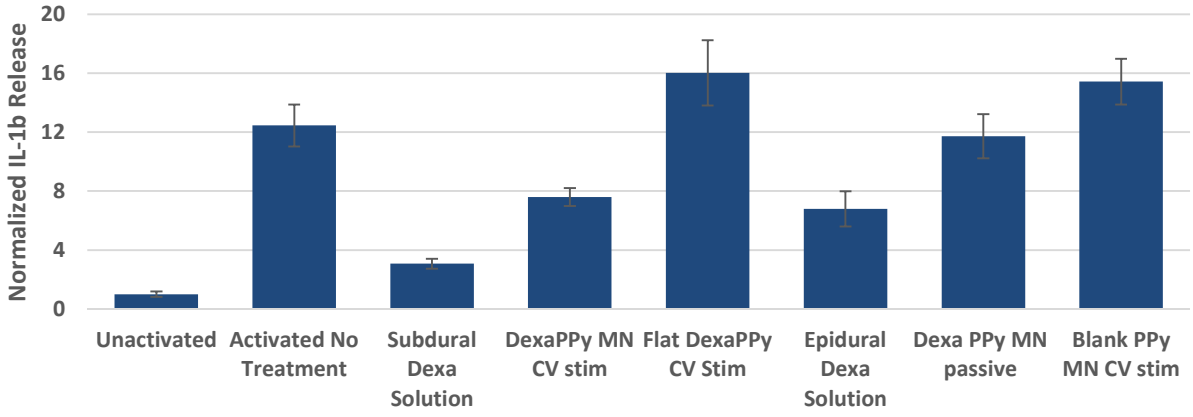
Normalized IL-1b Release
20
16
12
8
4
0
Unactivated
Activated No Treatment
Subdural Dexa Solution
DexaPPy MN CV stim
Flat DexaPPy CV Stim
Epidural Dexa Solution
Dexa PPy MN passive
Blank PPy MN CV stim

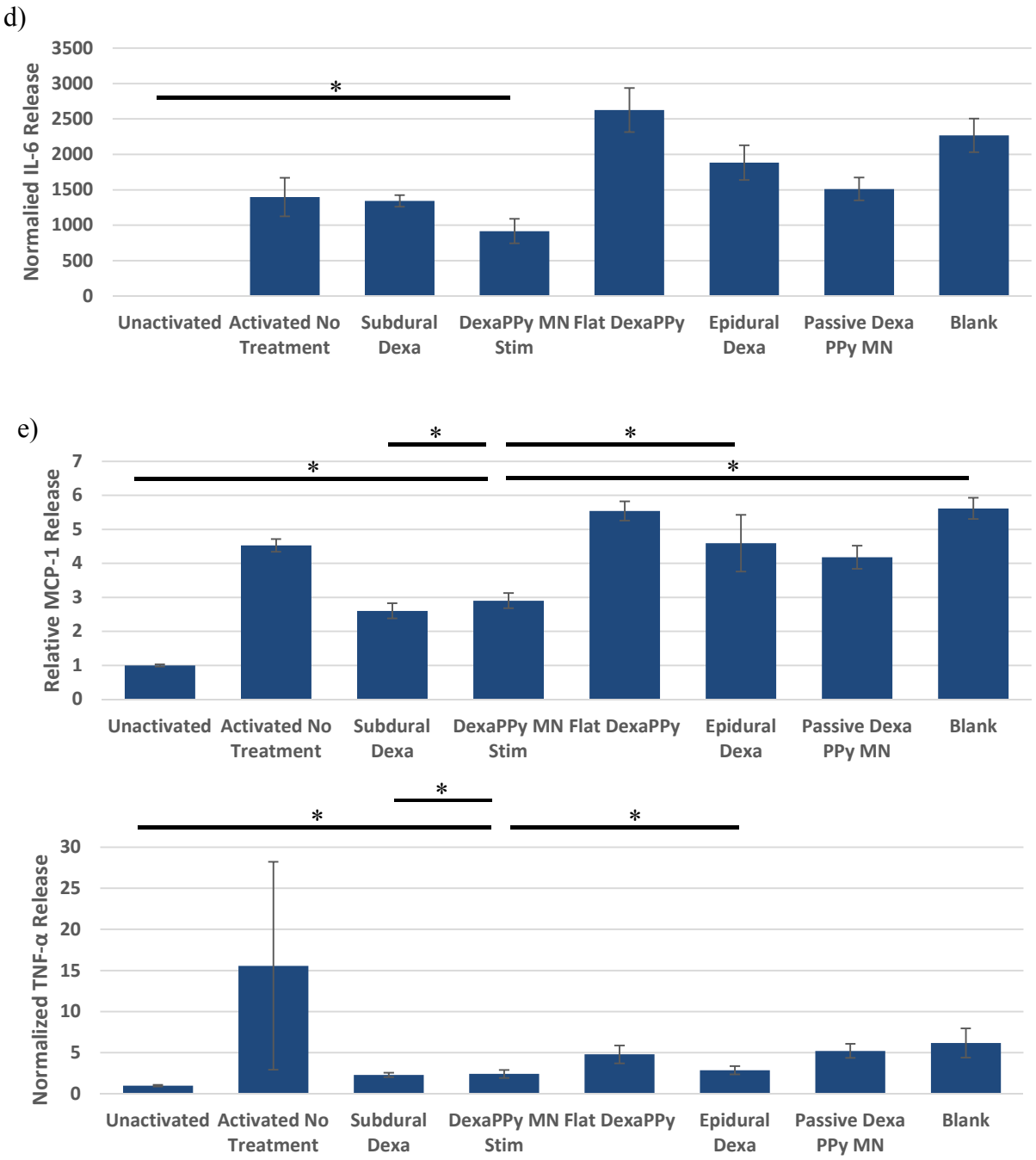

Figure 3.8. Neuroinflammation assays following transdural treatment of CV stimulated Dexa PPy microneedles.

a) MTS quantified relative cell viability in each treatment group. Release of b) NO, c) IL-1β, d) IL-6, e) MCP-1, f) TNF-α. (* $p < 0.05$ against CV stimulated Dexa PPy microneedles).

Chapter 4. CONCLUSION

The challenges of drug delivery for spinal cord injuries have motivated the design of a transdural electrically controlled microneedle array. The electrical control of delivery is implemented through the use of conductive polymer PPy. In this work, the PPy microneedle array is tested for use in transdural as well as electronically controlled release of a model drug dexamethasone phosphate. Quantification of transdurally released Dexa from electrically stimulated Dexa PPy microneedles demonstrate the ability of the microneedles in allowing transdural release of drugs unable to passively diffuse through the membrane. Use of the microneedles allowed subdural release of the drug with minimal damage to the dura, and minimal disruption in the subdural space. The release of Dexa on electrical stimulation additionally allows the external control of drug release after the application off the microneedles. Application of transdural, electrically stimulated release from the microneedles to *in vitro* neuroinflammation show bioactivity of the released Dexa. CV stimulated release from the microneedles was not seen to cause significant cell death. Transdural release of Dexa from the PPy microneedles using CV stimulation demonstrate promise in attenuating neuroinflammation, a mechanism of secondary spinal cord injury that may worsen the injury. Further investigations of Dexa PPy microneedles in the treatment of spinal cord injury may include in vivo tissue responses to the implanted material, as well as degradation of the material.

While this work uses dexamethasone phosphate to investigate transdural release from the PPy microneedles, a variety of pharmaceutical compounds may be loaded and released from PPy[36], including protein therapeutics [37, 38]. Future works may investigate the application of PPy microneedles in the transdural release of other neuroprotective compounds.

Chapter 5. REFERENCES

[1] National Spinal Cord Injury Statistical Center, Facts and Figures at a Glance, University of Alabama at Birmingham, Birmingham, AL, 2018.
[2] H.M. Gibbons, M. Dragunow, Microglia induce neural cell death via a proximity-dependent mechanism involving nitric oxide, Brain Res 1084(1) (2006) 1-15.
[3] Paralysis statistics, 2019. https://www.christopherreeve.org/living-with-paralysis/stats-about-paralysis.
[4] C.A. Oyinbo, Secondary injury mechanisms in traumatic spinal cord injury: a nugget of this multiply cascade, Acta Neurobiol Exp (Wars) 71(2) (2011) 281-99.
[5] D.J. Donnelly, P.G. Popovich, Inflammation and its role in neuroprotection, axonal regeneration and functional recovery after spinal cord injury, Exp Neurol 209(2) (2008) 378-88.
[6] E. Park, A.A. Velumian, M.G. Fehlings, The role of excitotoxicity in secondary mechanisms of spinal cord injury: a review with an emphasis on the implications for white matter degeneration, J Neurotrauma 21(6) (2004) 754-74.
[7] M.G. Fehlings, C.H. Tator, R.D. Linden, The relationships among the severity of spinal cord injury, motor and somatosensory evoked potentials and spinal cord blood flow, Electroencephalogr Clin Neurophysiol 74(4) (1989) 241-59.
[8] X.Z. Liu, X.M. Xu, R. Hu, C. Du, S.X. Zhang, J.W. McDonald, H.X. Dong, Y.J. Wu, G.S. Fan, M.F. Jacquin, C.Y. Hsu, D.W. Choi, Neuronal and glial apoptosis after traumatic spinal cord injury, J Neurosci 17(14) (1997) 5395-406.
[9] E. Emery, P. Aldana, M.B. Bunge, W. Puckett, A. Srinivasan, R.W. Keane, J. Bethea, A.D. Levi, Apoptosis after traumatic human spinal cord injury, J Neurosurg 89(6) (1998) 911-20.
[10] M.G. Fehlings, A. Vaccaro, J.R. Wilson, A. Singh, W.C. D, J.S. Harrop, B. Aarabi, C. Shaffrey, M. Dvorak, C. Fisher, P. Arnold, E.M. Massicotte, S. Lewis, R. Rampersaud, Early versus delayed decompression for traumatic cervical spinal cord injury: results of the Surgical Timing in Acute Spinal Cord Injury Study (STASCIS), PLoS One 7(2) (2012) e32037.
[11] B.C. Walters, M.N. Hadley, R.J. Hurlbert, B. Aarabi, S.S. Dhall, D.E. Gelb, M.R. Harrigan, C.J. Rozelle, T.C. Ryken, N. Theodore, Guidelines for the management of acute cervical spine and spinal cord injuries: 2013 update, Neurosurgery 60(CN_suppl_1) (2013) 82-91.
[12] M.L. Gill, P.J. Grahn, J.S. Calvert, M.B. Linde, I.A. Lavrov, J.A. Strommen, L.A. Beck, D.G. Sayenko, M.G.V. Straaten, D.I. Drubach, D.D. Veith, A.R. Thoreson, C. Lopez, Y.P. Gerasimenko, V.R. Edgerton, K.H. Lee, K.D. Zhao, Neuromodulation of lumbosacral spinal networks enables independent stepping after complete paraplegia, Nature Medicine 24(11) (2018) 1677-1682.
[13] M.L. Gill, P.J. Grahn, J.S. Calvert, M.B. Linde, I.A. Lavrov, J.A. Strommen, L.A. Beck, D.G. Sayenko, M.G. Van Straaten, D.I. Drubach, D.D. Veith, A.R. Thoreson, C. Lopez, Y.P. Gerasimenko, V.R. Edgerton, K.H. Lee, K.D. Zhao, Neuromodulation of lumbosacral spinal networks enables independent stepping after complete paraplegia, Nat Med 24(11) (2018) 1677-1682.
[14] I. Lavrov, C.J. Dy, A.J. Fong, Y. Gerasimenko, G. Courtine, H. Zhong, R.R. Roy, V.R. Edgerton, Epidural Stimulation Induced Modulation of Spinal Locomotor Networks in Adult Spinal Rats, (2008).
[15] M. Zurita, J. Vaquero, S. Oya, C. Morales, Effects of dexamethasone on apoptosis-related cell death after spinal cord injury, J Neurosurg 96(1 Suppl) (2002) 83-9.
[16] B.K. Kwon, W. Tetzlaff, J.N. Grauer, J. Beiner, A.R. Vaccaro, Pathophysiology and pharmacologic treatment of acute spinal cord injury, Spine J 4(4) (2004) 451-64.
[17] M.B. Bracken, W.F. Collins, D.F. Freeman, M.J. Shepard, F.W. Wagner, R.M. Silten, K.G. Hellenbrand, J. Ransohoff, W.E. Hunt, P.L. Perot, Jr., et al., Efficacy of methylprednisolone in acute spinal cord injury, Jama 251(1) (1984) 45-52.
[18] M.B. Bracken, M.J. Shepard, W.F. Collins, T.R. Holford, W. Young, D.S. Baskin, H.M. Eisenberg, E. Flamm, L. Leo-Summers, J. Maroon, et al., A randomized, controlled trial of methylprednisolone or naloxone in the treatment of acute spinal-cord injury. Results of the Second National Acute Spinal Cord Injury Study, N Engl J Med 322(20) (1990) 1405-11.
[19] M.B. Bracken, M.J. Shepard, T.R. Holford, L. Leo-Summers, E.F. Aldrich, M. Fazl, M. Fehlings, D.L. Herr, P.W. Hitchon, L.F. Marshall, R.P. Nockels, V. Pascale, P.L. Perot, Jr., J. Piepmeier, V.K. Sonntag, F. Wagner, J.E. Wilberger, H.R. Winn, W. Young, Administration of methylprednisolone for 24 or 48 hours or tirilazad mesylate for 48 hours in the treatment of acute spinal cord injury. Results of the Third National Acute Spinal Cord Injury Randomized Controlled Trial. National Acute Spinal Cord Injury Study, Jama 277(20) (1997) 1597-604.
[20] M.N. Hadley, B.C. Walters, P.A. Grabb, N.M. Oyesiku, G.J. Przybylski, D.K. Resnick, T.C. Ryken, Pharmacological therapy after acute cervical spinal cord injury, Neurosurgery 50(3 Suppl) (2002) S63-72.
[21] M.D. Baumann, C.E. Kang, C.H. Tator, M.S. Shoichet, Intrathecal delivery of a polymeric nanocomposite hydrogel after spinal cord injury, Biomaterials 31(30) (2010) 7631-9.
[22] T.S. Wilems, S.E. Sakiyama-Elbert, Sustained dual drug delivery of anti-inhibitory molecules for treatment of spinal cord injury, J Control Release 213 (2015) 103-11.
[23] A. Jain, Y.T. Kim, R.J. McKeon, R.V. Bellamkonda, In situ gelling hydrogels for conformal repair of spinal cord defects, and local delivery of BDNF after spinal cord injury, Biomaterials 27(3) (2006) 497-504.
[24] G. Perale, F. Rossi, M. Santoro, M. Peviani, S. Papa, D. Llupi, P. Torriani, E. Micotti, S. Previdi, L. Cervo, E. Sundstrom, A.R. Boccaccini, M. Masi, G. Forloni, P. Veglianese, Multiple drug delivery hydrogel system for spinal cord injury repair strategies, J Control Release 159(2) (2012) 271-80.
[25] Y.T. Kim, J.M. Caldwell, R.V. Bellamkonda, Nanoparticle-mediated local delivery of Methylprednisolone after spinal cord injury, Biomaterials 30(13) (2009) 2582-90.
[26] D. Gupta, C.H. Tator, M.S. Shoichet, Fast-gelling injectable blend of hyaluronan and methylcellulose for intrathecal, localized delivery to the injured spinal cord, Biomaterials 27(11) (2006) 2370-9.
[27] P.M. George, A.W. Lyckman, D.A. LaVan, A. Hegde, Y. Leung, R. Avasare, C. Testa, P.M. Alexander, R. Langer, M. Sur, Fabrication and biocompatibility of polypyrrole implants suitable for neural prosthetics, Biomaterials 26(17) (2005) 3511-9.
[28] L. Leprince, A. Dogimont, D. Magnin, S. Demoustier-Champagne, Dexamethasone electrically controlled release from polypyrrole-coated nanostructured electrodes, J Mater Sci Mater Med 21(3) (2010) 925-30.
[29] R. Wadhwa, C.F. Lagenaur, X.T. Cui, Electrochemically controlled release of dexamethasone from conducting polymer polypyrrole coated electrode, J Control Release 110(3) (2006) 531-41.
[30] C. Boehler, C. Kleber, N. Martini, Y. Xie, I. Dryg, T. Stieglitz, U.G. Hofmann, M. Asplund, Actively controlled release of Dexamethasone from neural microelectrodes in a chronic in vivo study, Biomaterials 129 (2017) 176-187.

[31] W. Gao, J. Li, J. Cirillo, R. Borgens, Y. Cho, Action at a Distance: Functional Drug Delivery Using Electromagnetic-Field-Responsive Polypyrrole Nanowires, Langmuir 30(26) (2014) 7778-88.
[32] H. B., X. Yao, L. Zhang, Zhou, Dexamethasone Sodium Phosphate Attenuates Lipopolysaccharide-Induced Neuroinflammation in Microglia BV2 Cells, Naunyn-Schmiedeberg's archives of pharmacology (2020).
[33] T. Ogata, Y. Nakamura, K. Tsuji, T. Shibata, K. Kataoka, Steroid hormones protect spinal cord neurons from glutamate toxicity, Neuroscience 55(2) (1993) 445-9.
[34] Dr, R.L. A., J.E. Sim, M.A. Hayward, D.A. Wink, S.M. Martin, G.R. Buettner, Spitz, A Spectrophotometric Method for the Direct Detection and Quantitation of Nitric Oxide, Nitrite, and Nitrate in Cell Culture Media, Analytical biochemistry 281(2) (2000).
[35] T.S. W., R. Ramasamy, M. Abdullah, Vidyadaran, Inhibitory Effects of Palm α-, γ- And δ-Tocotrienol on Lipopolysaccharide-Induced Nitric Oxide Production in BV2 Microglia, Cellular immunology 271(2) (2011).
[36] D. Ge, X. Tian, R. Qi, S. Huang, J. Mu, S. Hong, S. Ye, X. Zhang, D. Li, W. Shi, A polypyrrole-based microchip for controlled drug release, Electrochimica Acta 55(1) (2009) 271-275.
[37] P.M. George, D.A. LaVan, J.A. Burdick, C.Y. Chen, E. Liang, R. Langer, Electrically Controlled Drug Delivery from Biotin-Doped Conductive Polypyrrole, Advanced Materials 18(5) (2006) 577-581.
[38] Y.C. Borgens, S. Riyi, I. Albena, B. Richard, A mesoporous silica nanosphere-based drug delivery system using an electrically conducting polymer - IOPscience, (2009).

APPENDIX A

Nanoindentor SEM Video

17.3nm/sec to max 10um:

https://drive.google.com/file/d/1vByw7AW7ReLTffvxKRh0mSTxOWoyk71q/view?usp=sharing

75um/sec to max 20um:

https://drive.google.com/file/d/13hg9WVO_YvhG5BULFY_cXUUWxQNskS0n/view?usp=sharing

150nm/sec to max 35um:

https://drive.google.com/file/d/1cNnQBBqa8Q9n7aw-xVcAjOIqWP1J95ts/view?usp=sharing

500nm/sec to max 35um:

https://drive.google.com/file/d/1cNQv4VzL-Jj-oBS_snvx0hTZKjlwUG2p/view?usp=sharing